

# A Method of Dual-Bias Voltage Supply for Reducing Reflection Loss in Reconfigurable Intelligent Surfaces of Liquid Crystal

Yue Cui, *Graduate Student Member, IEEE*, Hiroyasu Sato, *Member, IEEE*, Kai-Da Xu, *Senior Member, IEEE*, Hideo Fujikake, *Senior Member, IEEE*, and Qiang Chen, *Senior Member, IEEE*

**Abstract**—In this letter, we proposed a new method of dual-bias voltage supply for reducing reflection loss (RL) in reconfigurable intelligent surfaces of liquid crystal (RIS-LC). By independently controlling the resonances of two dipoles biased by two different voltages, a one-to-multiple correspondence between reflection phase and magnitude is established. Consequently, the RL can be minimized by selecting the optimal reflection magnitude for each reflection phase. For demonstration, a  $12 \times 13$  array of RIS-LC is fabricated and measured. The experimental results show that the proposed RIS-LC achieves a maximum reflection magnitude of  $-0.7$  dB with a reflection phase range of  $570^\circ$  at 41 GHz. It validates the proposed method can significantly reduce the RL without sacrificing reflection phase range. The presented RIS-LC possesses the advantages of simple structure, low cost and ease of fabrication.

**Index Terms**—Liquid crystal (LC), low cost, millimeter wave, reconfigurable intelligent surface (RIS), reflection loss.

## I. INTRODUCTION

SIXTH-GENERATION (6G) wireless communication needs base station antennas with high gain and high frequency (millimeter-wave and above) for high data speed and large communication capacity [1]. However, these requirements also suffer from some challenges such as narrow beamwidth and coverage hole existence. Reconfigurable intelligent surface (RIS) offers a potential solution to these issues, which has the capability of controlling the electromagnetic (EM) wave propagation [2]. RIS serves as an effective method to enhance the electromagnetic (EM) signal level within a target area by shaping the beam, which can adapt to the evolving complexities of coverage requirements [3]. Due to its two-dimensional structure, it also facilitates seamless integration with the facades and interior walls of buildings.

Numerous studies on RIS have been explored so far, including RIS controlled by diodes [4]–[6], mechanical methods [7]–[9] and nematic liquid crystal (LC) [10]–[15]. The nematic LC is composed of rod-shaped molecules that can be reoriented

by an external electric field, resulting in continuous adjustment of its permittivity. This characteristic of LC enables the reconfigurable intelligent surface of liquid crystal (RIS-LC) to seamlessly shift the beam direction, representing its primary advantage. Additionally, applying an external electric field to the LC through a bias line is a straightforward process, which can simplify the design of RIS-LC with low cost.

On the contrary, LC materials usually exhibit high loss tangent, which significantly leads to notable reflection loss (RL). [15]. RL refers to the dissipation of partially incident EM wave energy, resulting in a reduction of the reflection magnitude and aperture efficiency of RIS-LC [16]. Several studies have focused on minimizing the RL of RIS-LC [15], [17], [18]. An alternative approach is using a loss-suppression structure to decrease the electric field within the LC layer, thereby reducing RL [15]. Another strategy is increasing the thickness of the LC layer to achieve the same objective [17]. Additionally, RL can be minimized by designing resonant structures to alter the impedance of RIS-LC [18]. However, these methods will lead to increased complexity or cost of the RIS-LC and inevitably result in a reduction of the reflection phase range.

In this letter, a novel RIS-LC unit cell using a dual-bias voltage supply method is proposed. Two bias lines are introduced to control the LC permittivities beneath two dipoles with different sizes, thereby enabling independent control of each dipole's resonance. Through this approach, one reflection phase can correspond to multiple reflection magnitudes, allowing for the selection of optimal magnitudes across all phases. Consequently, the proposed RIS-LC can achieve a reduction of RL without compromising the phase range, while maintaining a simple structure.

## II. STRUCTURE AND ANALYSIS

The proposed structure of the RIS-LC unit cell is depicted in Fig. 1(a) and 1(b), comprising a superstrate layer, an LC layer, and a metal ground. Two dipoles connected to bias lines are located between the superstrate and the LC layer. This arrangement enables independent control of the resonance states of the two dipoles via two different bias voltages ( $V_1$  and  $V_2$ ). The schematics of the LC molecules biased by voltages  $V_1$  and  $V_2$  are illustrated in Fig. 1(c) and 1(d), respectively. Since the LC molecule is rugby ball shaped, its long axis can be

This work was supported by the Ministry of Internal Affairs and Communications in Japan (JPJ000254). (Corresponding author: Kai-Da Xu)

Yue Cui, Hiroyasu Sato, Kai-Da Xu and Qiang Chen are with the Department of Communications Engineering, Tohoku University, Sendai 980-8579, Japan. (e-mail: cui.yue.t4@dc.tohoku.ac.jp, sahiro@ecei.tohoku.ac.jp, kaidaxu@ieee.org, qiang.chen.a5@tohoku.ac.jp)

Hideo Fujikake is with the Department of Electronic Engineering, Tohoku University, Sendai 980-8579, Japan. (e-mail: hideo.fujikake.e6@tohoku.ac.jp)

considered as a director for the LC permittivity ( $\epsilon_{rLC}$ ). In the proposed RIS-LC, the director of the LC molecules is aligned in the y-direction by polyimide films with micro-grooves in the same direction, which are coated on both the superstrate and the metal ground. When the bias voltage  $V_1$  is supplied, the LC molecules beneath the right dipole are deflected towards the z-direction, thereby changing the LC relative permittivity  $\epsilon_{r1}$  in this region, as shown in Fig. 1(c). Similarly, the LC relative permittivity in the left region  $\epsilon_{r2}$  will be changed when the bias voltage  $V_2$  is supplied, as illustrated in Fig. 1(d). The corresponding relative permittivities and loss tangents of LC are  $\epsilon_{r\perp} = 2.5$  and  $\tan \delta_{\perp} = 0.02$  under no bias voltage, and  $\epsilon_{r\parallel} = 3$  and  $\tan \delta_{\parallel} = 0.01$  under full bias voltage (40 V in the proposed design), respectively. For the superstrate material, non-alkali glass ( $\epsilon_{rG} = 5.4$ ,  $\tan \delta = 0.007$ ) is chosen due to its smooth surface, which facilitates the polyimide film coating process.

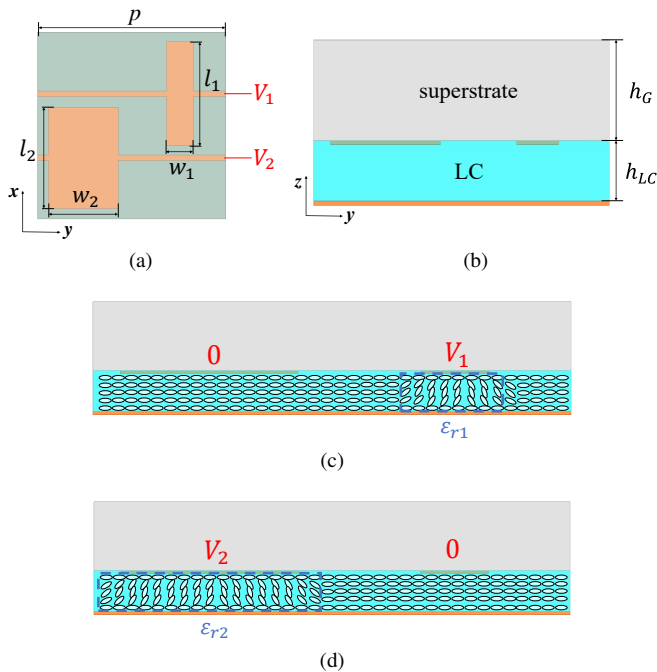


Fig. 1. (a) Top view and (b) side view of the proposed RIS-LC unit cell structure. Schematics of the LC molecules under (c) only bias voltage  $V_1$  and (d) only bias voltage  $V_2$ . The parameters are  $p=3.5$  mm,  $l_1=1.95$  mm,  $w_1=0.5$  mm,  $l_2=1.9$  mm,  $w_2=1.3$  mm,  $h_G=0.5$  mm, and  $h_{LC}=0.05$  mm.

For a RIS using array of resonant unit cells, the reflection phase is manipulated by altering the resonance of unit cell [19]. The proposed RIS unit cell introduces two microstrip dipoles as the resonant structure, whose resonant frequency can be calculated as [20]:

$$(f)_{mn} = \frac{1}{2\pi\sqrt{\mu_0\epsilon_0\epsilon_{re}}} \sqrt{\left(\frac{m\pi}{l}\right)^2 + \left(\frac{n\pi}{w}\right)^2} \quad (1)$$

where the  $l$  and the  $w$  represent the length and width of the dipole, respectively. The  $m$  and the  $n$  denote the resonant mode numbers. The  $\epsilon_{re}$  is the equivalent relative permittivity that can be approximated as [21]:

$$\epsilon_{re} = \frac{\epsilon_{rG} + \epsilon_{rLC}}{2} + \frac{\epsilon_{rG} - \epsilon_{rLC}}{2} \left(1 + 12 \frac{h_{LC}}{l}\right)^{-\frac{1}{2}} \quad (2)$$

where  $\epsilon_{rG}$  and  $\epsilon_{rLC}$  represent the relative permittivities of the non-alkali glass and LC, respectively. Since  $\epsilon_{rLC}$  can be manipulated by an external electric field, the resonance of the proposed RIS-LC unit cell can be altered by supplying different bias voltages. To ensure a significant phase change when adjusting the bias voltages, two distinct dipoles are incorporated into the proposed unit cell.

For RIS-LC biased by a single voltage, the permittivity of the LC remains unchanged across all resonant structures within a unit cell. Consequently, this results in a one-to-one correspondence between the reflection coefficient and the LC permittivity (or bias voltage) [18], [22], [23]. Fig. 2 illustrates the performance of the proposed RIS-LC through full-wave simulation under single-bias voltage, where  $V_1 = V_2$  and  $\epsilon_{r1} = \epsilon_{r2}$ . The frequency response of the reflection coefficients is depicted in Fig. 2(a). It is evident that the resonant frequencies will be decreased as the permittivity of the LC increases, resulting in changes in reflection magnitude and phase at a single frequency point. Fig. 2(b) displays the variations of reflection magnitude and phase for different LC permittivities at 41 GHz. As can be seen, the proposed RIS-LC unit cell exhibits a phase variation of  $570^\circ$ , but with high RL (up to 19 dB) where the phase changes rapidly. It is worth noting that one reflection phase corresponds to only one LC permittivity, consequently corresponding to one reflection magnitude. Usually, there is a trade-off between the RL and phase range [15]. Therefore, designing a RIS-LC unit cell structure with low RL and large phase range simultaneously under single-bias voltage is very challenging.

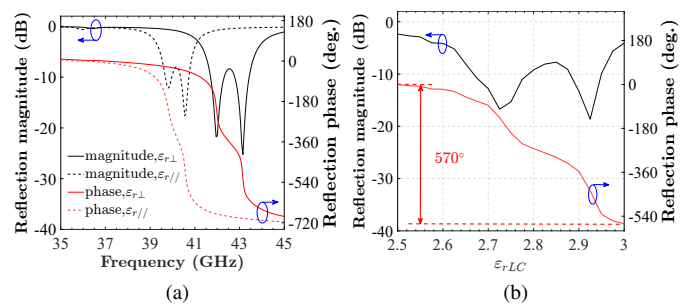


Fig. 2. Simulated reflection coefficient (a) versus frequency and (b) versus  $\epsilon_{rLC}$  at 41 GHz under single-bias voltage.

In order to effectively solve this issue, the proposed RIS-LC unit cell is introduced with two bias lines, enabling the control of reflection magnitude and phase through dual-bias voltage. It is similar to the design principle of Cassegrain antenna or Gregorian antenna, where the introduction of a sub-reflector enables magnitude and phase correction to reduce side lobes and improve cross-polarization [24], [25]. The introduction of an additional bias voltage also enables relatively independent control of the reflection magnitude and phase of RIS-LC. Simulated reflection magnitude and phase at 41 GHz under the dual-bias voltage are depicted in Fig. 3. It is evident that the reflection phase and magnitude exhibit a one-to-multiple correspondence for the LC permittivity. This behavior is attributed to the independent control of  $\epsilon_{r1}$  and  $\epsilon_{r2}$  facilitated by the dual-bias voltage. The reflection phase range is almost

the same as the single-bias voltage, and the introduction of dual-bias voltage allows one phase mapped to multiple value sets of  $(\epsilon_{r1}, \epsilon_{r2})$ . Consequently, the optimal reflection magnitude can be chosen from these value sets to obtain low RL.

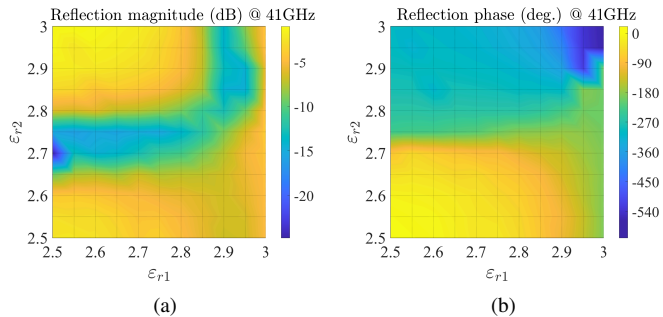


Fig. 3. Simulated (a) reflection magnitude and (b) reflection phase at 41 GHz under dual-bias voltage.

The effect of reducing RL through dual-bias voltage is demonstrated in Fig. 4. The relationship between the reflection coefficient and LC permittivity at 41 GHz is depicted using a Smith chart. The red line and blue dots indicate reflection coefficients under single-bias voltage ( $\epsilon_{r\perp} \leq \epsilon_{r1} = \epsilon_{r2} \leq \epsilon_{r\parallel}$ ) and dual-bias voltage ( $\epsilon_{r\perp} \leq \epsilon_{r1} \leq \epsilon_{r\parallel}$ ,  $\epsilon_{r\perp} \leq \epsilon_{r2} \leq \epsilon_{r\parallel}$ ), respectively. It can be seen that the variation of the reflection coefficient covers a region on the Smith chart under dual-bias voltage. Moreover, this region encompasses the red line, indicating that a higher reflection magnitude can be chosen by dual-bias voltage across almost all phases. Selecting the envelope within this region of the reflection coefficient effectively minimizes RL due to the LC. Furthermore, the region of reflection coefficient could be expanded by employing LC with a large variation range of permittivity or increasing the number of bias voltage supply.

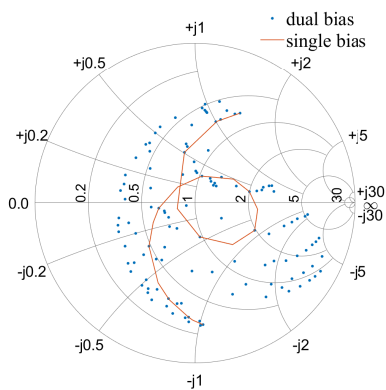


Fig. 4. Simulated reflection coefficient comparisons between single- and dual-bias voltages at 41 GHz.

### III. MEASUREMENT

For demonstration, a  $12 \times 13$  array of RIS-LC prototype has been fabricated, as illustrated in Fig. 5(a). The electrodes of the two types of dipoles are positioned on the right and left sides of the array, with bias voltages of  $V_1$  and  $V_2$  through

flexible feed lines, respectively. Fig. 5(b) and 5(c) display the unit cell under a microscope when the bias voltages  $V_1$  and  $V_2$  are individually applied, respectively. It can be seen that the area around the two dipoles brightens separately. This phenomenon occurs because the directors of the LC molecules in these regions are deflected to the  $z$  direction by the bias voltage, enabling incident light to pass through and be reflected by the ground. It is evident that the bias voltages  $V_1$  and  $V_2$  can control the relative permittivities of LC beneath the two dipoles, i.e.,  $\epsilon_{r1}$  and  $\epsilon_{r2}$ , respectively. The reflection coefficient and phase range of the prototype RIS-LC array were measured by lens-loaded printed antipodal fermi tapered slot antenna (APFA) [26] using Keysight Network Analyzer P5008A, as shown in Fig. 5(d). The low-frequency bias voltages  $V_1$  and  $V_2$  are generated by a computer-controlled NF Multifunction Generator WF1974 and amplified by NF High Speed Power Amplifier 4005.

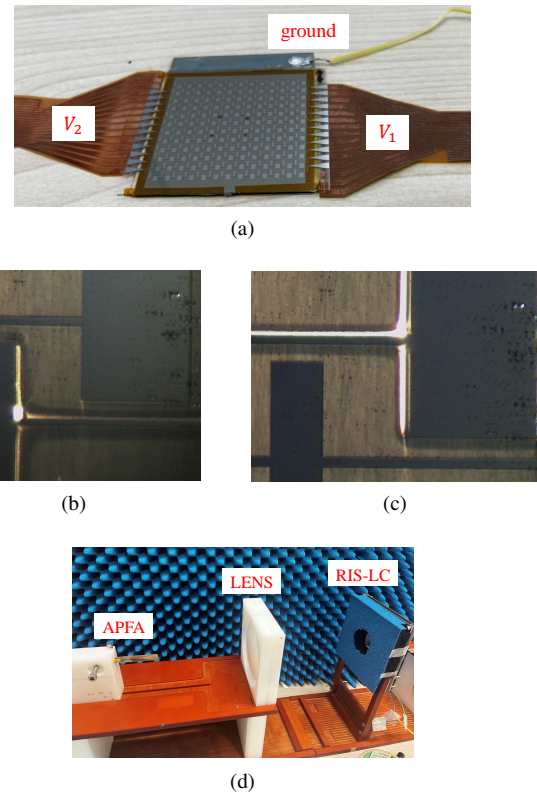


Fig. 5. (a) Prototype of the proposed RIS-LC array, reactions of LC under microscope at bias voltages (b)  $V_1$  and (c)  $V_2$ , and (d) measurement environment.

Fig. 6 illustrates the measured reflection magnitude and phase of the proposed RIS-LC array at 41 GHz under single- and dual-bias voltages. For the single-bias voltage, the reflection phase range is  $570^\circ$  and the minimum reflection magnitude is 24 dB at 41 GHz, as shown in Fig. 6(a) and 6(b). Fig. 6(c) and 6(d) represent the relationship between reflection coefficient and dual-bias voltage. The phase range and magnitude variations are the same as those for single-bias voltage, consistent with the previous theoretical analysis. Since one reflection phase corresponds to multiple magnitudes under dual-bias voltage, the optimal magnitude could be chosen to reduce the RL.

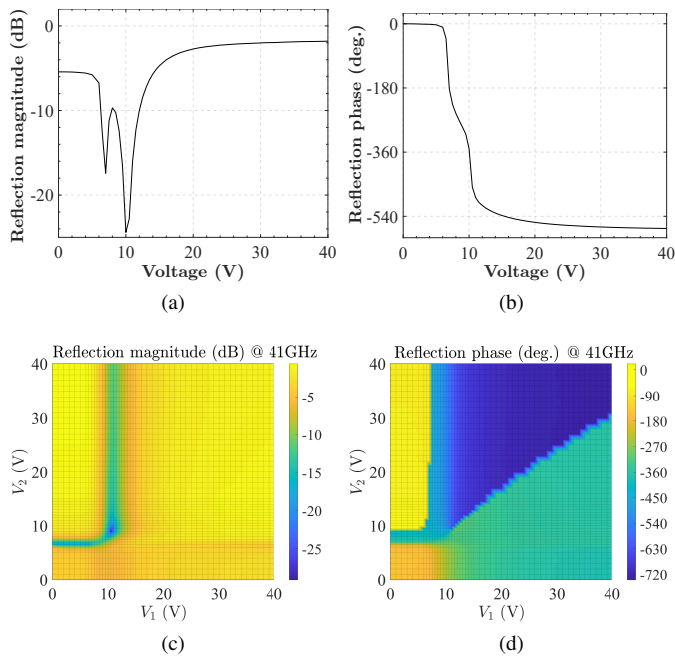


Fig. 6. Measured (a) reflection magnitude and (b) reflection phase at 41 GHz under single-bias voltage. (c) Reflection magnitude and (d) reflection phase at 41 GHz under dual-bias voltage.

Fig. 7(a) presents a comparison of reflection coefficients at 41 GHz under single- and dual-bias voltages using Smith chart. It is evident that the red line of the reflection coefficient under single-bias voltage is encompassed within the region under dual-bias voltage, which is consistent with the simulation results. Across the full  $360^\circ$  phase, a higher reflection magnitude can be observed in the region of the reflection coefficient under dual-bias voltage compared to single-bias voltage, thereby reducing RL without compromising phase range. For instance, at  $-43^\circ$  as depicted in Fig. 7(a), the reflection magnitude is  $-12.4$  dB under single-bias voltage and only  $-1.3$  dB under dual-bias voltage, resulting in a significant reduction of RL by 11.1 dB. The reflection magnitudes corresponding to phase under single- and dual-bias voltages at 41 GHz are depicted in Fig. 7(b), where the magnitudes represent the optimal values chosen at each phase. Across the full  $360^\circ$  phase, it is evident that the reflection magnitude under dual-bias voltage surpasses that under single-bias voltage, with a maximum difference of 17 dB. Measurement results indicate that the method of dual-bias voltage supply achieves significant reduction in RL, compared to the conventional single-bias voltage across all reflection phases.

Table I presents the performance comparisons of the proposed RIS-LC with other previous works. As can be seen, the proposed RIS-LC features a thin LC layer and simple structure, making it cost-effective and ease of fabrication. Moreover, compared to conventional single-bias voltage type, the proposed dual-bias voltage supply method introduces an additional degree of freedom for controlling the reflection coefficient, thereby enabling magnitude compensation of RIS-LC. The measured results validate the effectiveness of the proposed structure in reducing RL while unaffected the reflection

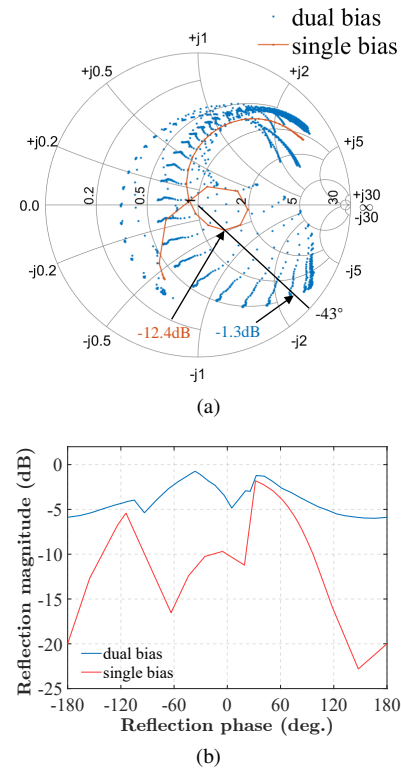


Fig. 7. Measured (a) reflection coefficient and (b) reflection magnitude and phase correspondence at 41 GHz under single and dual-bias voltage.

TABLE I  
COMPARISONS WITH PRIOR WORKS

Feature	[12]	[15]	[17]	[18]	This work
Frequency (GHz)	10	40.3	10	10	41
LC thickness( $\mu\text{m}$ )	500	100	500	250	50
Max. RL (dB)	37	6	6	3.5	5.6
Min. RL (dB)	5	3.4	-	0.7	0.48
Max. RL reduction(dB)	-	11.3	2	6	17
Phase range (deg.)	221	210	170	240	570

phase range.

#### IV. CONCLUSION

This letter proposed a novel dual-bias voltage supply method to reduce the RL of RIS-LC. Theoretical analysis reveals that the dual-bias voltage control the resonances of the two dipoles separately, enabling relatively independent control of the reflection magnitude and phase of RIS-LC. Under dual-bias voltage control, one reflection phase can correspond to multiple reflection amplitudes, allowing for RL reduction by selecting the optimal magnitude. A  $12 \times 13$  prototype array of the proposed RIS-LC design is fabricated and measured, whose results indicate effective reduction of RL without sacrificing the reflection phase range. Due to its simple structure and thin LC layer, the proposed RIS-LC can be readily used for future 6G applications.

## REFERENCES

- [1] W. Saad, M. Bennis, and M. Chen, "A vision of 6g wireless systems: Applications, trends, technologies, and open research problems," *IEEE Network*, vol. 34, no. 3, pp. 134–142, 2020.
- [2] E. Basar, M. Di Renzo, J. De Rosny, M. Debbah, M.-S. Alouini, and R. Zhang, "Wireless communications through reconfigurable intelligent surfaces," *IEEE Access*, vol. 7, pp. 116 753–116 773, 2019.
- [3] Q. Wu and R. Zhang, "Intelligent reflecting surface enhanced wireless network via joint active and passive beamforming," *IEEE Trans. Wireless Commun.*, vol. 18, no. 11, pp. 5394–5409, 2019.
- [4] W. Wu, K.-D. Xu, Q. Chen, T. Tanaka, M. Kozai, and H. Minami, "A wideband reflectarray based on single-layer magneto-electric dipole elements with 1-bit switching mode," *IEEE Trans. Antennas Propag.*, vol. 70, no. 12, pp. 12 346–12 351, 2022.
- [5] J. Han, L. Li, G. Liu, Z. Wu, and Y. Shi, "A wideband 1 bit  $12 \times 12$  reconfigurable beam-scanning reflectarray: Design, fabrication, and measurement," *IEEE Antennas Wireless Propag. Lett.*, vol. 18, no. 6, pp. 1268–1272, 2019.
- [6] X. Cao, Q. Chen, T. Tanaka, M. Kozai, and H. Minami, "A 1-bit time-modulated reflectarray for reconfigurable-intelligent-surface applications," *IEEE Trans. Antennas Propag.*, vol. 71, no. 3, pp. 2396–2408, 2023.
- [7] W. Menzel, D. Pilz, and M. Al-Tikriti, "Millimeter-wave folded reflector antennas with high gain, low loss, and low profile," *IEEE Antennas Propag. Mag.*, vol. 44, no. 3, pp. 24–29, 2002.
- [8] X. Yang, S. Xu, F. Yang, M. Li, H. Fang, Y. Hou, S. Jiang, and L. Liu, "A mechanically reconfigurable reflectarray with slotted patches of tunable height," *IEEE Antennas Wireless Propag. Lett.*, vol. 17, no. 4, pp. 555–558, 2018.
- [9] A. Hu, K. Konno, Q. Chen, and T. Takahashi, "A highly efficient 1-bit reflectarray antenna using electromagnet-controlled elements," *IEEE Trans. Antennas Propag.*, vol. 72, no. 1, pp. 506–517, 2024.
- [10] S. Bildik, S. Dieter, C. Fritzsche, W. Menzel, and R. Jakoby, "Reconfigurable folded reflectarray antenna based upon liquid crystal technology," *IEEE Trans. Antennas Propag.*, vol. 63, no. 1, pp. 122–132, 2015.
- [11] X. Li, Y. Wan, J. Liu, D. Jiang, T. Bai, K. Zhu, J. Zhuang, and W.-Q. Wang, "Broadband electronically scanned reflectarray antenna with liquid crystals," *IEEE Antennas Wireless Propag. Lett.*, vol. 20, no. 3, pp. 396–400, 2021.
- [12] M. Y. Ismail, R. Cahill, M. Amin, A. F. M. Zain, and M. K. Amin, "Phase range analysis of patch antenna reflectarray based on nematic liquid crystal substrate with dynamic rcs variation," in *2007 Asia-Pacific Microwave Conference*, 2007, pp. 1–4.
- [13] W. Hu, R. Cahill, J. A. Encinar, R. Dickie, H. Gamble, V. Fusco, and N. Grant, "Design and measurement of reconfigurable millimeter wave reflectarray cells with nematic liquid crystal," *IEEE Trans. Antennas Propag.*, vol. 56, no. 10, pp. 3112–3117, 2008.
- [14] X. Li, H. Sato, H. Fujikake, and Q. Chen, "Development of two-dimensional steerable reflectarray with liquid crystal for reconfigurable intelligent surface application," *IEEE Trans. Antennas Propag.*, pp. 1–1, 2024.
- [15] Y. Cui, H. Sato, Y. Shibata, T. Ishinabe, H. Fujikake, and Q. Chen, "A low-cost structure for reducing reflection loss in intelligent reflecting surface of liquid crystal," *IEEE Antennas Wireless Propag. Lett.*, vol. 22, no. 12, pp. 3027–3031, 2023.
- [16] P. Nayeri, F. Yang, and A. Z. Elsherbeni, *Reflectarray antennas: theory, designs, and applications*. John Wiley & Sons, 2018.
- [17] M. Ismail and R. Cahill, "Application of liquid crystal technology for electronically scanned reflectarrays," in *2005 Asia-Pacific Conference on Applied Electromagnetics*, 2005, pp. 82–85.
- [18] H. Kim, J. Kim, and J. Oh, "Liquid-crystal-based x-band reactively loaded reflectarray unit cell to reduce reflection loss," *IEEE Antennas Wireless Propag. Lett.*, vol. 20, no. 10, pp. 1898–1902, 2021.
- [19] D. Pozar, S. Targonski, and H. Syrigos, "Design of millimeter wave microstrip reflectarrays," *IEEE Trans. Antennas Propag.*, vol. 45, no. 2, pp. 287–296, 1997.
- [20] C. A. Balanis, *Antenna theory: analysis and design*. John Wiley & sons, 2016.
- [21] I. J. Bahl, "Build microstrip antennas with paper-thin dimensions," *Microwaves*, vol. 18, p. 50, 1979.
- [22] J. Yang, X. Chu, H. Gao, P. Wang, G. Deng, Z. Yin, and H. Lu, "Fully electronically phase modulation of millimeter-wave via comb electrodes and liquid crystal," *IEEE Antennas Wireless Propag. Lett.*, vol. 20, no. 3, pp. 342–345, 2021.
- [23] G. Perez-Palomino, P. Baine, R. Dickie, M. Bain, J. A. Encinar, R. Cahill, M. Barba, and G. Toso, "Design and experimental validation of liquid crystal-based reconfigurable reflectarray elements with improved bandwidth in f-band," *IEEE Trans. Antennas Propag.*, vol. 61, no. 4, pp. 1704–1713, 2013.
- [24] P. Hannan, "Microwave antennas derived from the cassegrain telescope," *IRE Transactions on Antennas and Propagation*, vol. 9, no. 2, pp. 140–153, 1961.
- [25] F. Holt and E. Bouche, "A gregorian corrector for spherical reflectors," *IEEE Trans. Antennas Propag.*, vol. 12, no. 1, pp. 44–47, 1964.
- [26] H. Sato, Y. Takagi, and K. Sawaya, "High gain antipodal fermi antenna with low cross polarization," *IEICE transactions on communications*, vol. 94, no. 8, pp. 2292–2297, 2011.